

Research Article

Properties of Adobe Bricks Manufactured from Vertisol Reinforced with Brewer's Spent Grains: Case Study in Sudano Sahelian Region of Cameroon

Viviane Bakainé Djaoyang^{1,2,*} , **Maxime Dawoua Kaoutoing³** ,
Bertin Pagna Kagonbé², Colbert Babé¹, Bernard Kola⁴, Noël Djongyang¹

¹Department of Renewable Energy, National Advanced School of Engineering of Maroua, University of Maroua, Maroua, Cameroon

²Local Materials Promotion Authority, Yaoundé, Cameroon

³National Advanced School of Mines and Petroleum Industries, University of Maroua, Kaélé, Cameroon

⁴Energy Research Laboratory, Institute for Geological and Mining Research, Yaoundé, Cameroon

Abstract

This paper presents the results of an investigation in establishing the physical and mechanical properties of brewer spent grain which have been used in the fabrication of Adobe. The earth block reinforced 2. 4. 6. 8 and 10 percent of brewer spent grain. The characteristics of raw material were investigated using X-ray diffraction (XRD) and FTIR analysis spectra show kaolinite, smectite and quartz. The clay materials are mainly composed of silica SiO₂ and alumina Al₂O₃ and these two oxides. The blocks, after 21 days of curing were tested for density, water absorption, compressive strength, tensile strength, and erosion resistance. It was found that the brewer's spent grain content slightly improved the blocks' density. The linear shrinkage decreases with brewer-spent grain additions from 0 - 10% allowing in 53%. The thermal conductivity decreases when the brewer spent grain the content of 60% is observed for the adobe containing 10 wt% brewer spent grain. The good compressive strength of the adobes incorporating brewer spent grain, their good resistance to water erosion and their low thermal conductivity shows that, these composites can be used in the building of individual habitats in the sub-Saharan zone.

Keywords

Adobes Bricks, Brewer Spent Grain, Clay Material, Thermal Conductibility, Building, Cameroon

1. Introduction

Due to the steadily rising energy costs of various building materials, it is necessary to switch back to using ecologically friendly materials that are abundant and inexpensive to produce [1]. Mineral resources found in abundance in the sub-

surface have long been used to build habitats [2]. Concrete's recent popularity can be attributed to both its perceived modernity and objective factors like durability, good mechanical characteristics and standardized implementation techniques.

*Corresponding author: vivibakiane@gmail.com (Viviane Bakaine Djaoyang)

Received: 16 January 2025; **Accepted:** 3 February 2025; **Published:** 21 February 2025



Copyright: © The Author(s), 2025. Published by Science Publishing Group. This is an **Open Access** article, distributed under the terms of the Creative Commons Attribution 4.0 License (<http://creativecommons.org/licenses/by/4.0/>), which permits unrestricted use, distribution and reproduction in any medium, provided the original work is properly cited.

Earth is one of the oldest and most widespread construction material [1]. Currently, it is estimated that about 30% of the world's population lives in earth buildings [3]. In most developing countries, houses are essentially constructed using locally produced adobes [4]. In light of this, the building industry must adapt its construction methods to provide novel materials that satisfy the updated user and regulatory standards for comfort, environmental impact and health [5, 6].

Earthen materials are readily available [8], recyclable [9], have high thermal and acoustic qualities [10] are fire resistant [7], and are less expensive than other building materials [10], earthen materials are occasionally chosen. Furthermore, there are no CO₂ emissions from the primary earthy material manufacturing process [11]. According to the literature review, several writers emphasize the practicality of certain fibers in buildings, such as the fibers from agave, date palm tree surfaces, and eucalyptus globulus leaves [12-14] and calotropis procera fibers [15]. Other authors in previous works especially on earth bricks using natural fibers as reinforcements concern alfa fibers [16], banana fibers [20], millet waste [21].

Concerning compressive strength, for instance, the stabilized soil blocks/bricks outperformed the unstabilized ones in all of these trials, with improvements ranging from 4% to 117% (median of 26%) [9].

Developing countries, particularly those in Asia, which do not have adequate wood supplies use straws and other non-wood materials as lignocellulosic fiber sources for pulp and paper production [24]. Lignocellulosic, including agricultural wastes and agro-industrial by-products. The major constituents of brewer's spent grain are cellulose, hemicellulose and lignin. However, it should be noted that spent grain is

an important source of pollution, as it is discharged into the environment and water.

This study aims to valorize local resources, namely earth material and brewer spent grain. We investigate the mechanical, physical and mineralogy characteristics of adobe bricks stabilized by adding brewer's wasted grain wastes to accomplish this goal.

2. Material and Experimental Procedures

2.1. Geographical and Geological Setting

The geographical location of the study is presented in Figure 1. Administratively, the study was conducted in Salak and Katoual namely Profile Salak Gaklé (PSG), Salak Engrenage (PSE) and Katoual (PSL). These localities are situated in Maroua I Subdivision, Diamaré Division, in Far North region of Cameroon (Figure 1). There are two distinct seasons in the Sudan-Sahelian climate: a wet season from June to September and a dry season from November to May [26]. Overall basins combined, the average annual rainfall is 671.6 mm yr⁻¹. The average annual temperature is 31.1°C, with the warmest months being March and April (28.6 and 28.7 °C, respectively), and the coldest months being December and January (27-26°C) (Table 1). The vertisol type mainly constitutes soils in these areas. The Sahelian savanna, or steppe, serves as vegetation cover. However, due to significant human degradation, crops including rice, corn, millet, onions, and sorghum have taken its place [27].

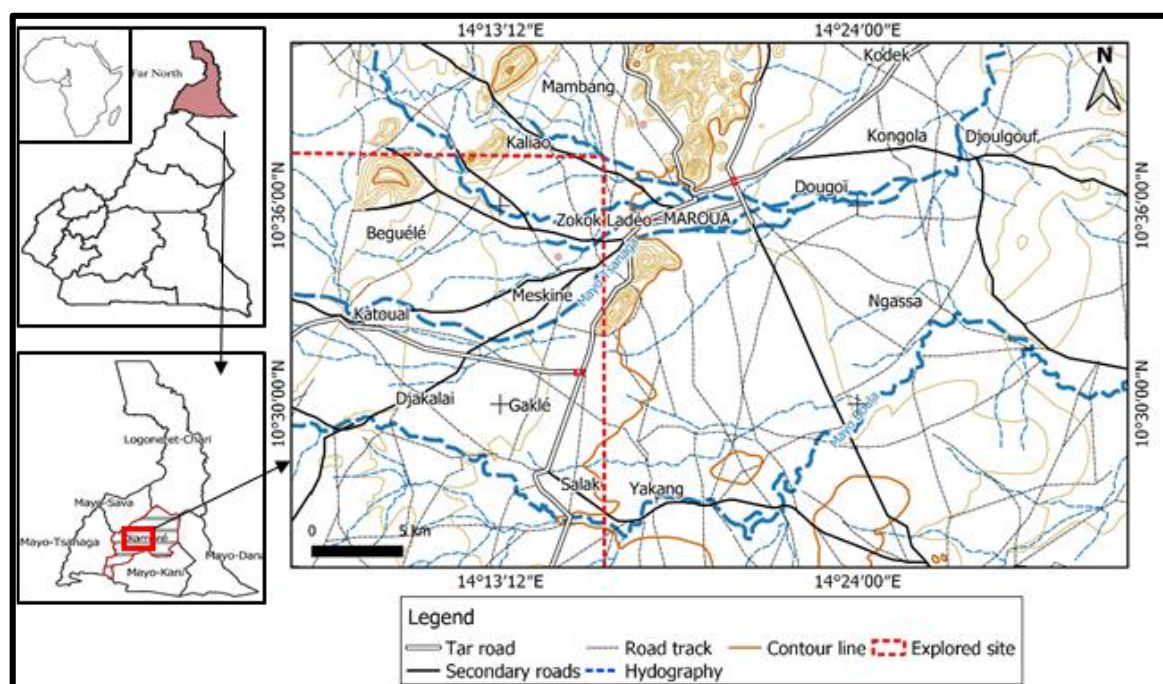


Figure 1. Location of the study area.

Table 1. Climatic data of the studied area.

| Station | Par | Jan | Feb | Mar | Apr | May | Jun | Jul | Aug | Sep | Oct | Nov | Dec | Average |
|---------|--------|------|-----|------|------|------|-------|-------|-------|------|------|------|------|---------|
| Maroua | P (mm) | 0 | 0 | 3.7 | 20.6 | 62.9 | 134.3 | 215.9 | 241.3 | 15.9 | 30.1 | 0.35 | 0 | 866.05 |
| | T (°C) | 26.9 | 29 | 32.8 | 33 | 33.9 | 30.2 | 28.6 | 27.6 | 28.2 | 29.7 | 29.1 | 27.3 | 30 |

2.2. Field Work and Sample Collection

Field missions included soil surveys, ambient condition reports and firsthand observations to determine pit placement. Two localities (Salak and Katoual) were further retained for detailed investigation. Three raw materials samples were from various sites: two samples from Salak (PSG and PSE) and one sample from Katoual (PSL) (Figure 2b).

The additions of brewer's leftover grain used here to add strength to the adobes came from the brewer in Garoua in North Cameroon (Figure 2a) presents dried brewer's spent grain. The brew's spent grain used in the experiments is produced with maize Gritz, malt, and yeast. The chemical composition, defined as a percentage of dry weight (w/w), was graciously provided and presented. 4.6% ashes, 15.2% proteins, 5.8% extractives, 1.4% acetyl groups, 16.8% cellulose, 28.4% hemicellulose, and 27.8% lignin [25].



Figure 2. Raw material (a), Brewer's spent grain (b).

2.3. Methods of Experiments

2.3.1. Manufacture of Adobe

Using an agate mortar, the clayey soil was crushed into particles of various sizes < 5 mm after being dried at 105, and the brewer's spent grain was dried in the ambient air. Dried raw clay powder was combined with six different weight percentages of dried brewer's spent grain (0, 2, 4, 6, and 10% of the mixture).

The amount of water calculated above supplied a sufficient consistency for adobes made with clayey materials mixed with the brewer's remaining grain waste. To allow for the fermentation of brewer's spent grain waste, the resulting

pastes were homogenized for 15 minutes and then stored for 72 hours in hermetically sealed plastic.

The homogeneous pastes were put into $4 \times 4 \times 16$ cm³ molds in two layers as follows. The mold was half-filled with paste and then manually shocked 20 times. Similar to the specimen (20 x 20 x 2) cm³, the prismatic specimens used for certain physical tests were elaborate. The earth-rendering mortars were remolded and then stored for 21 days [23, 28, 29] (Figure 3).

The blocks have been tested for linear shrinkage, compressive strength, water absorption, and wearing and erosion. These studies were carried out in Cameroon at the Local Materials Promotion and Authority.



Figure 3. Specimens after demounting.

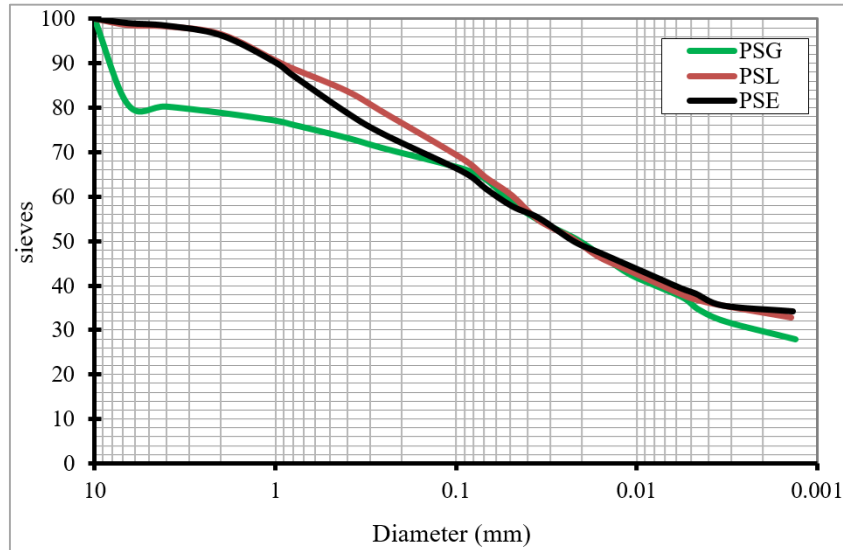


Figure 4. Granulometric Curves.

2.3.2. Physical, Chemical and Mineralogical Characterization of Raw Materials

Two methods were used to analyze the distribution of the soil mixtures: pipette analysis was used for the finer fraction (less than 80 μm) and wet sieving was used for the coarser fraction ($\geq 80 \mu\text{m}$) following standard NF P 94-057 (Figure 4). The geotechnical characteristics of the soils were determined by measuring the Atterberg limits according to the NF P94-051 standard. Infrared (IR) and X-ray diffraction (XRD) were used to evaluate the soils mineralogical. The chemical element/ composition of the soil was determined following

BS EN ISO 17294-1 [31, 32].

2.3.3. Adobes' Mechanical, Thermal and Physical Properties

The German standard [33] was followed to determine the linear shrinkages (in percentage) of the earth rendering mortars by comparing the starting and final lengths measured on the three prismatic specimens ($40 \times 40 \times 160 \text{ mm}^3$) before and after drying (Figure 5a). After drying at 105 $^{\circ}\text{C}$ for 24 hours, prismatic specimens ($40 \times 40 \times 40 \text{ mm}^3$) were used for the water absorption tests by capillarity of the specimen following EN 15801 CEN 2009 standard.

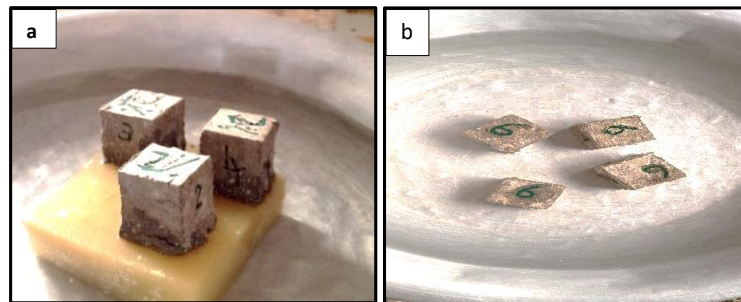


Figure 5. (a) Water absorption test by capillarity (b) Water absorption test by immersion.

The percentage of water absorption in the materials was calculated by the weight difference between the samples after immersion in water and the dry samples using the following equation [17, 30] (Figure 5a and 5b).

$$\text{Absorption } (\%) = \frac{m(t) - m_s}{m_s} \quad (1)$$

Where $m(t)$ The mass of the dry sample; m_s is the mass of the sample immersed in water.

To simulate the erosion impact of rain for 10 minutes at a flow rate of 5 L/min for erosion experiments. The spray is positioned around 120 mm in height above the sample. The coefficient of the erosion test is provided in the form of a percentage of material lost during the erosion test. Eq. (2) [23, 28]:

$$\text{CE} = \frac{(m_o - m_s)}{m_o} \times 100 \quad (2)$$

To measure the thermal conductivity, samples are first dried in an oven at 105°C for 48 h and then put in airtight plastic bags for 48 h to obtain a uniform temperature [23]. This work's objectives are to measure the volumetric heat capacity (ρC_p) and thermal effusivity experimentally, and then estimate the sample's thermal conductivity. To achieve this, we used a thermophysical characterization method of the asymmetrical hot plane. The full model numerical modeling, using pre-estimated beginning values E and ρC_p from the simplified model, demonstrates convergence between the model temperature and experimental temperatures. This convergence further justifies that the model developed is the thermo-physical properties of this material.

The thermal conductivity is obtained by:

$$\lambda = \frac{E^2}{\rho C_p} \text{ Or } \lambda = \frac{(E^2)_{est}}{(\rho C_p)_{est}} \quad (3)$$

A plane heating element having the same section (10 x 10 cm²) as the sample is placed under the sample. A heat flux step is sent into the heating element and the transient temperature $T(t)$ is recorded [22, 23, 40, 46, 47]. Moreover, this thermal contact resistance will be disregarded because polystyrene is an insulator (Figure 6). The method's basic idea is to estimate the sample's temperature and thermal capacity values in a way that minimizes the sum of square errors between the theoretical and experimental curves [46]. The quadratic error expression is provided by [46]:

$$\psi = \sum_{i=1}^n [\Delta T_{exp}(t_i) - T_{model}(t_i)]^2 \quad (4)$$

Where ψ is the quadratic error between experimental and theoretical values, T_{exp} is the experimental temperature, T_{model} is the theoretical temperature.

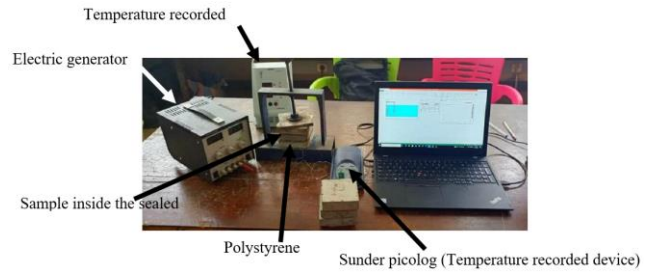


Figure 6. Asymmetrical hot-plane experimental device.

3. Results and Discussion

3.1. Physico-Properties of Raw Materials

3.1.1. Grain-size Distribution Behavior

Particle size distribution on clay samples from Salak and Katoul shows a variation in grain size (Table 1). The size distribution curve reveals that the sample PSG, PSL, and PSE, were composed of 21.2, 3.5, and 3.7 wt.% of coarse, 28.4; 45.8; 46.4 wt.% of sand (20-200 m), 20, 17.1, 15.1 wt.% of silt (2-20 m) and 29.5; 33.6; 34. wt. % of clay (<2 m) clay respectively. This high clayey fraction concentration is a component of the Vertisols [27, 34-36] diagram (Figure 7) used to analyze soil texture (2005); these soils are categorized as heavy sandy clay. The grading curves of the studied clays are reported in Figure 8. Grain size analysis enabled the establishment of grain curves which reveal similarities of these soils on one hand and differences on the other hand.

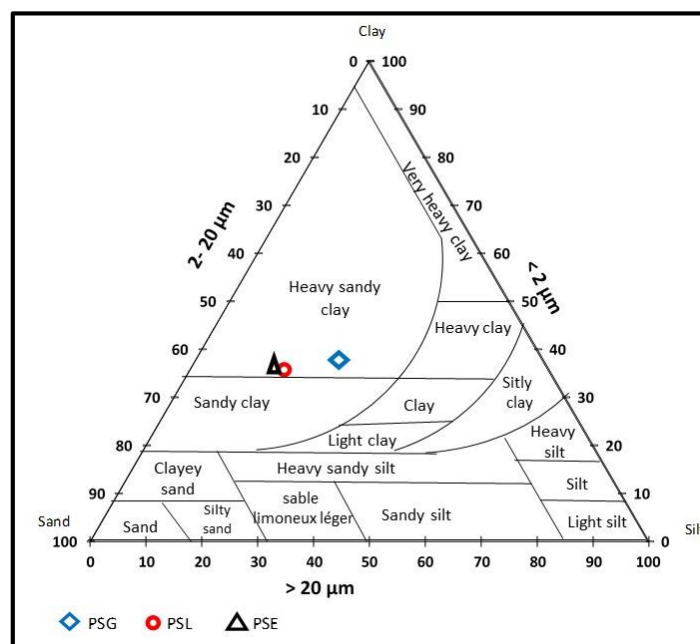


Figure 7. Position of Salak and Katoul clay materials in empirical diagrams for textures (Richer de Forges et al., 2008).

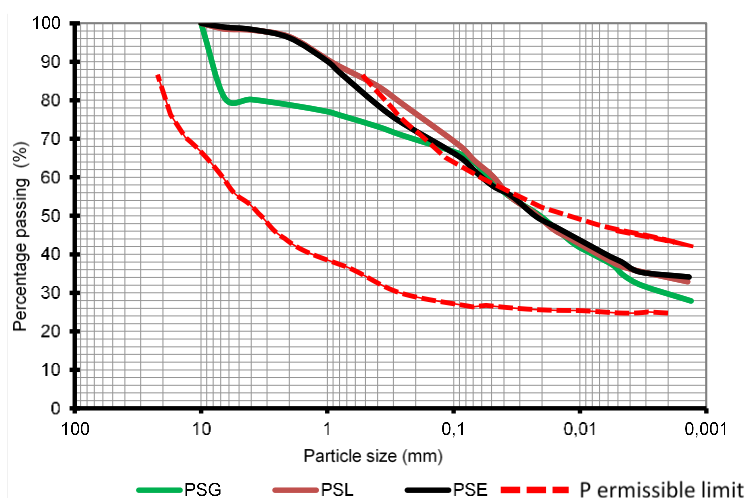


Figure 8. Plotting the granulometric curves of the investigated soils next to the grading envelope of soil materials used to make earth brick (XP P 13-901, 2001).

3.1.2. Plasticity of Raw Materials

Table 2 shows that the soil under investigation had a liquid limit (WL), plastic limit (WP), and plasticity index (PI) of 42.6-49.8%, 20.7-24.4%, and 21.9-25.4%, respectively according to Standard NFP 94-051. As specified by the International Center for Earth Construction, CRATerre-EAG, re-

ported by [37], the liquid limit and the plasticity index are indicated in the diagram shown in Figure 9. This plasticity index of this material allows it to be classified as medium plastic and falls in groups A – 7– 6 (AASHTO system) or considered as CH (USCS system) (Figure 9). The limits of the recommended zones are approximate

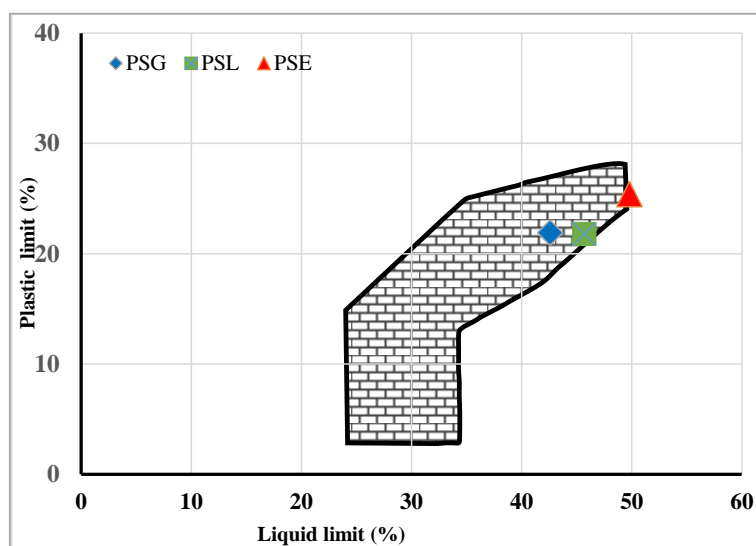


Figure 9. Recommended plasticity spindles for building with BTC and Adobe according to French standards [Norme-NF-XP-P13-901, 2001].

3.2. Characterization Mineralogical and Chemical of the Soil

3.2.1. Geochemical Composition

The geochemical analysis of major elements was carried out by X-ray Fluorescence on tree samples. The findings are

reported in Table 2. It made it possible to determine the percentage of oxides silica, titanium Alumina, iron oxides, magnesium, manganese, calcium, sodium, potassium, and P_2O_5 . In all studied samples, the predominant oxide is Silica SiO_2 (55.99-66.35%), Alumina Al_2O_3 (12.82-15.00%), and Fe_2O_3 , (5.86-7.88). There is a correlation between the presence of clay minerals and the values of alumina and iron oxide. [38]. The alkalis are represented by K_2O (2.32-4.33) and

Na₂O (0.48-1.01) thus indicating their very weak character or even traces of these elements in the material. Accepted PSL (0.92%) sample CaO contents > 1% indicate the presence of a source of CaO other than plagioclase (Chahi and Petit, 2002) [39]. These probably come from the calcite, materialized by the limestone nodules observed in the field. Constituents such

as MnO, P₂O₅, and TiO₂ are found in trace amounts in all samples. The ratio of SiO₂/ Al₂O₃ is > 4.08 and ranges from 4.08 to 5.17, indicating excess silica content. According to Tsozué *et al* and Nguetnkam *et al.* [38, 40], the relatively high SiO₂/Al₂O₃ ratios observed are related to a different degree of weathering and reflect the presence of 2:1-type clays.

Table 2. Physical and chemical characteristics of soils the Salak and Katoual in weight percentages.

| | Samples | | |
|--|---------|-------|-------|
| | PSG | PSL | PSE |
| Clay: (<0.002 mm) | 29.5 | 33.6 | 34.8 |
| Silt: (0.002-0.02 mm) | 20.9 | 17.1 | 15.1 |
| Sand: (0.02-2 mm) | 28.4 | 45.8 | 46.4 |
| Gravel: (>2 mm) | 21.2 | 3.5 | 3.7 |
| Liquid limit (LL) | 42.6 | 45.7 | 49.8 |
| Plastic limit (PL) | 20.7 | 22.1 | 24.4 |
| Plastic index (PI) | 21.9 | 21.8 | 25.4 |
| SiO ₂ | 61.28 | 66.35 | 61.23 |
| Al ₂ O ₃ | 15.00 | 12.82 | 12.63 |
| Fe ₂ O ₃ | 7.88 | 5.86 | 7.08 |
| Mn ₂ O ₃ | 0.21 | 0.14 | 0.13 |
| MgO | 0.86 | 0.62 | 0.89 |
| CaO | 1.59 | 0.92 | 4.06 |
| Na ₂ O | 0.48 | 1.00 | 1.01 |
| K ₂ O | 2.32 | 4.33 | 3.93 |
| TiO ₂ | 1.23 | 1.17 | 1.22 |
| P ₂ O ₅ | 0.02 | 0.03 | 0.01 |
| L.O.I | | | |
| SiO ₂ /Al ₂ O ₃ | 4.08 | 5.17 | 4.84 |

3.2.2. Mineralogical Composition

The XRD patterns of the studied samples are reported in Figure 10. This X-ray diagram shows the presence of smectite (15.68 Å), kaolinite (7.15 Å), quartz (3.24 Å, 2.45 Å, 2.28 Å, 2.23 Å, 1.15 Å, 1.98 Å, 1.81 Å, 1.67 Å, and 1.65 Å), illite (9.96 Å) and feldspar (4.25 Å). Globally, this mineralogical composition is similar to that obtained in Benue floodplain clays [41-43], Logone Valley clays and Lake Chad Basin clay in Central Africa [27], and Maroua clays [44], in Soudano-Sahelian areas of Cameroon. These materials' increased plasticity index can be at least partially explained by the presence of smectite [32, 42]. Furthermore, it has been clearly

established that smectites contribute significantly to the instability of the mechanical characteristics of earth bricks. [37, 38, 45].

The IR spectrum of the raw material Figure 11. The first zone, which lies between 3696 and 3619 cm⁻¹, displays the distinctive bands of the kaolinite network's exterior hydroxyl bonds (OH) and potentially those of illites [48, 49]. Insufficiently crystallized kaolinite is indicated by the presence of two bands rather than four [30]. Al-OH vibration at 912 cm⁻¹, Si-O-Si vibration at 766 and 692 cm⁻¹ in quartz, and 1626 cm⁻¹ in hygroscopic water. The vibrations around 523 cm⁻¹ and 412-455 cm⁻¹ are, respectively, attributable to the deformations of the Si-O-Al IV and Si-O-Si bonds in the kao-

linite [27, 39, 45].

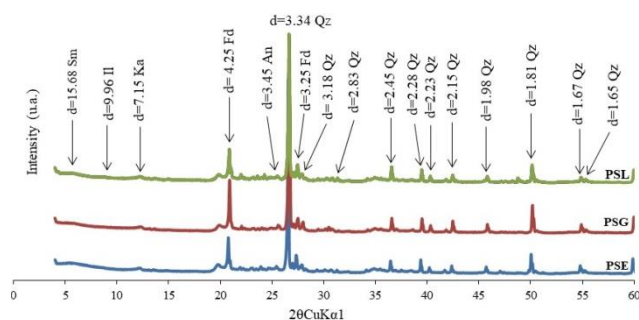


Figure 10. X-ray powder diffraction patterns of clay materials.

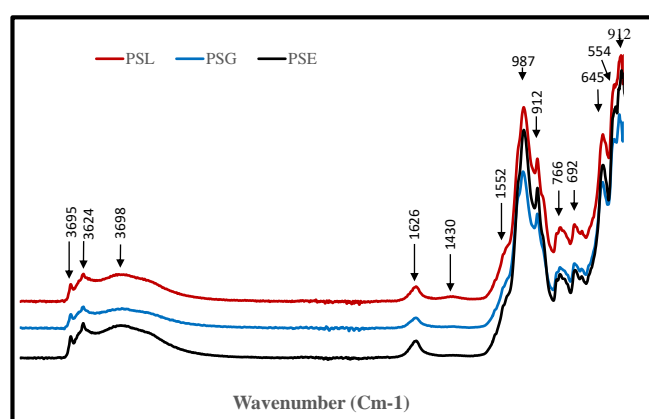


Figure 11. The IR spectrum of the raw material.

4. Impact of Stabilization on the Properties of Brick Specimens

4.1. Physical-mechanical Properties of Stabilized Brick Specimens

These bio-sourced composites' hydric nature is an important variable in why building construction can accept them. Through immersion or capillarity, the material's absorption of water is measured. [46]. After 10 minutes of partial submersion in water, the coefficient of water absorption is measured. As the spent grain percentage of a brew increases from 0% to 2%, the water absorption coefficient decreases, as seen in Figure 12, increases with the amount of spent grain in the brew above 2%, however, it still stays lower than in the unreinforced adobe samples. The numbers (2, 4, 6, 8, and 10%) in these examples indicate that there is increased waste of water into the adobes that aren't reinforced. Water absorption is limited by the presence of waste grain brewer in adobe bricks. It is used for building materials and adobe bricks can limit water absorption due to the fibers' activity [19, 28]. According to recent studies, the addition of these fibers to reinforced adobes improves durability and lowers the possi-

bility of cracks developing after drying [46].



Figure 12. Water absorption of adobes at different percentage.

The water absorption coefficient decreases with brew's spent grain additions Figure 11, which leads to the formation of insoluble amine silicate (hydrophobic molecule) which glues isolated particles together through chemical bonds, making adobe less permeable to water [29] Beyond 0.4 wt% of fonio straw, the formation of clusters and the increase in open porosity slows down the water absorption kinetics [2].

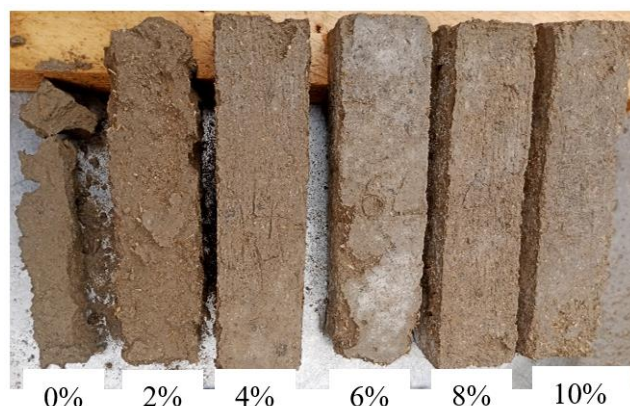


Figure 13. Aspect of adobe bricks after the erosion test.

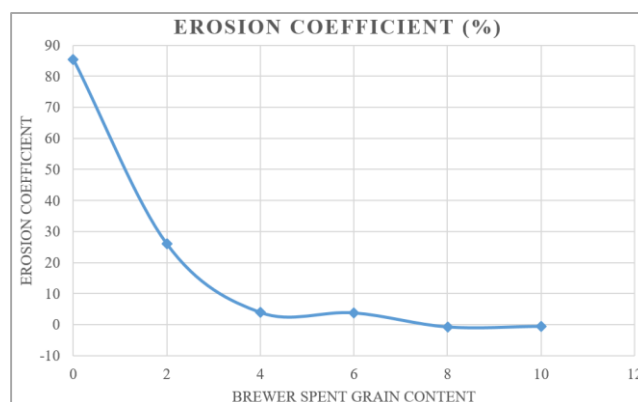


Figure 14. Erosion coefficient of adobes at different percentage.

The erosion coefficient of adobes decreases when the

brewer spent grain content increases Figure 13. The erosion coefficient was reduced by 97% with the adobes reinforced of 8 and 10% of the wastes compared to the unreinforced adobes Figure 14. In this percentage the adobes absorbed water. This behavior may be due to the good adhesion and distribution of waste within the soil matrix. [23]. These results can be explained by the formation of insoluble amine silicate, which binds the isolated particles of raw materials together [60]. The optimal adobes reinforced with brewer-spent grain is 4%.

The linear shrinkage of adobe mortars according to their brewer-spent grain is reported in Figure 15. The linear shrinkage decreases with brewer-spent grain additions from 0 -10% allowing in a 53%. This result is due to the good adhesion of brewer spent grain with the clayey matrix. Similar results have already been reported in the literature on raw earth plasters reinforced with plant fibers [47, 48].

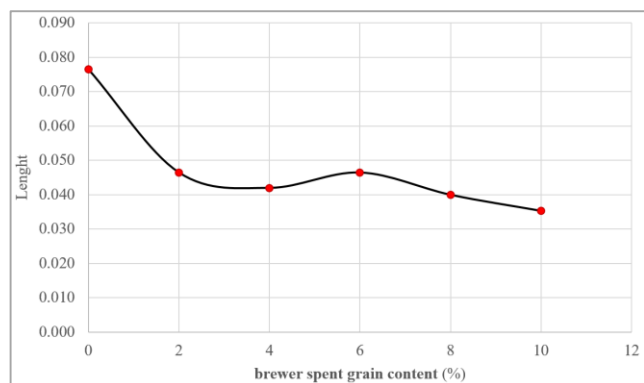


Figure 15. Linear shrinkages of adobes at different percentage.

Adobe bricks without stabilizers have a compressive strength of 6.8 MPa, as shown in Figure 16. This number is comparable to the compressive strength measured by Zak et al. [49] on adobes alone. Compared to reinforced with 2, 4, 6, and 8% fiber (6.8, 5.6, 5.4, and 4.9 MPa, respectively), its compressive strength is superior (Figure 17). The adobes reinforced by fibers of millet, the results show that the addition of fibers of millet by 2% decreased the compressive strength is 6.7. [23]. the effect of red-algae fibers on compressed earth bricks for construction, there are obtained the maximum strength was 4.07 MPa with the incorporation of 1.5 red-algae fibers [46]. The adobes are compliant with the normative ranges of tolerance concerning the minimum acceptable compressive strength of 2% set out by French norm XP 13-901, 2001. [23, 50]. This decreases to a level below maximal strength. The weak bond. This resemblance in mechanical strength between the brewer's spent grain and the clay is the reason for the strength, which stays below the maximum strength. A less-than-ideal bond between the brewer's spent grain and the clay matrix could be the cause of this. However, when 10% of the brewer's grain is used as reinforcement, the compressive strength of adobe bricks increases. His loss of mechanical strength was correlated with the increase in porosity due to the agglomeration of

brewer-spent grain for high brewer-spent grain contents [2, 29]. Likewise, at this percentage, the fibers strengthen and maintain the solid matrix, increase the bonding strength of the earth-fiber mixture and the appearance of cracks is greatly reduced [49, 56]. However, the lowest value of the compressive strength is 4.9 MPa and corresponds to the composition mixed with 4% of fibers which is much higher than those obtained by many authors in the literature [2, 18, 19, 23, 46, 49, 57, 58, 59].

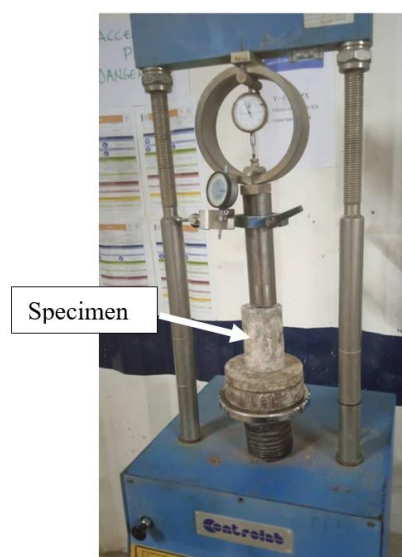


Figure 16. The test of compressive strength on adobes.

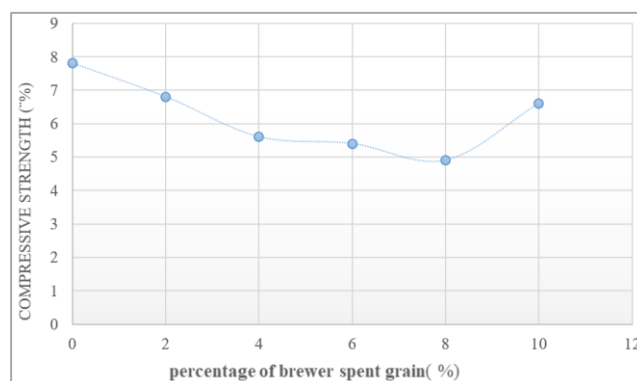


Figure 17. Compressive strength of adobes at different brewer spent grain contents.

4.2. Thermal Conductivity of Adobes

Figure 18 reported the evolution of thermal conductivity for dried samples as an addition of brewer spend grain amount. For brewer-spent grain contents of 0, 2, 4, 6, 8, and 10%, respectively, the thermal conductivity of adobe bricks reinforced with brewer-spent grain is 1.12; 0.93; 0.74; 0.66; 0.57, and 0.45 W/(mK). As compared to bricks without reinforcement brewer-spent grain, the previous results show that increasing the percentage of brewer-spent grain from 0% to 10%

allows for a 60% decrease in heat conductivity. Figure 18 reveals the change in thermal conductivity with brewer spent grain content. When the brewer spent grain increases, the thermal conductivity lowers. Furthermore, because fibers are lighter, they gradually substitute the ground volume, which lowers thermal conductivity. [23, 28, 52-54, 55]. Thermal

conductivity decreases the addition of barley straw and hemp [51]. The value of the thermal conductivity varies between 1.12; 0.93; 0.74; 0.66; 0.57, and 0.45 W/(m. K) respectively. This result proves that the addition of the brewer-spent grain contributes to improving thermal conductivity in the building with adobes.

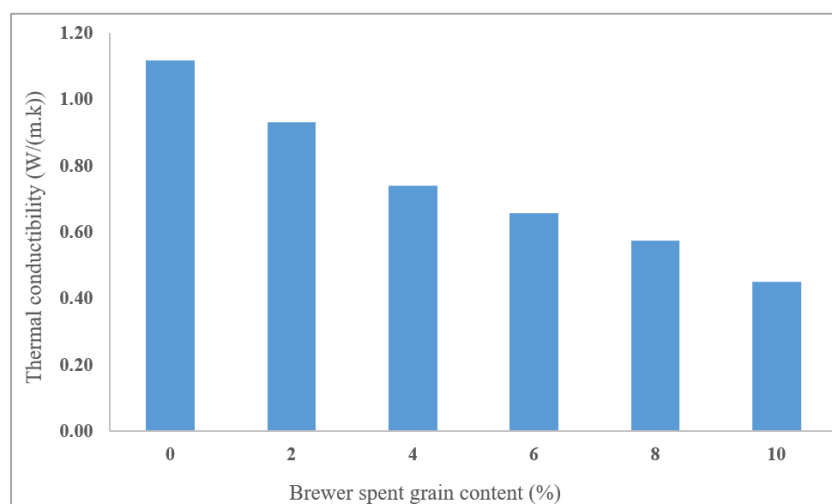


Figure 18. Thermal conductivity of adobes as a function of Brewer spent grain.

The $T=f(t)$ thermograms obtained from the complete model for sample MAT00 are shown in Figure 19. A low level of probe inertia is observed at the start of recording in Figure 19 (a) and (b). The rigorous non-convergence of the estimation residuals presented by green curves at the central zero can be explained by: the material still having a high water content; the surfaces of the material surfaces that are not smooth; high contact resistances; high roughnesses on the material surface.

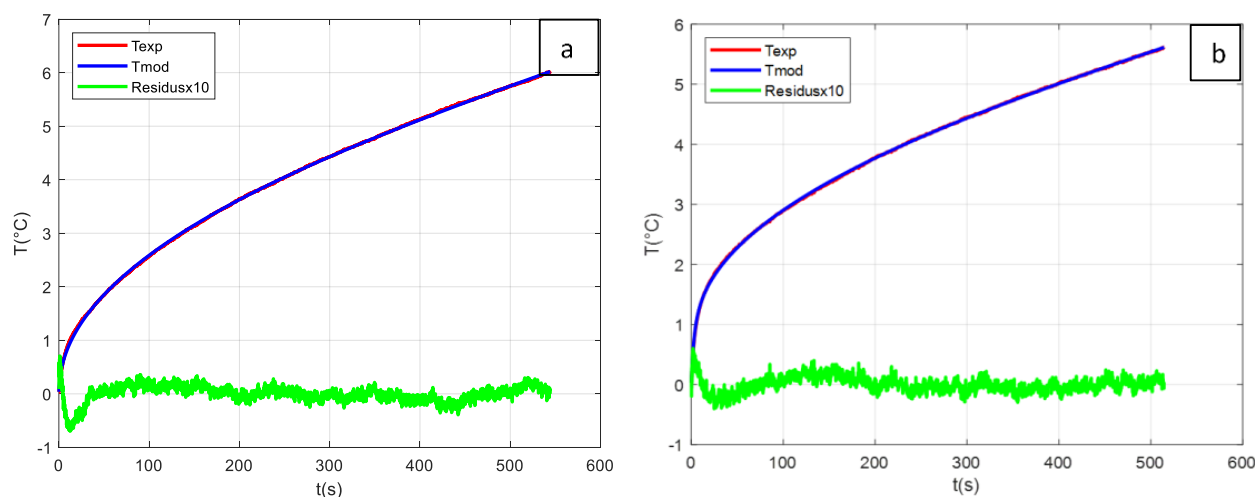


Figure 19. Experimental and modeled hot plate temperature obtained adobes: (a) unreinforced adobe (b) reinforced adobe (% brewer spent grains content).

5. Conclusion

The impact of brewer-spent grains on the microstructure,

the physical properties, and the mechanical characteristics of adobes manufactured with a clayey soil in Far Nord material for the manufacture of adobes showed that it was mainly composed of kaolinite quartz, smectic, and anatase. The clay materials are mainly composed of silica SiO_2 and alumina

Al₂O₃ and these two oxides the proportions relatively low. The soil used for adobe production has good geotechnical and particle size Characteristics. According to mechanical characterization, the compressive strength of adobe bricks manufactured with 0 and 2, 4, 6, 8, and 10% brewer waste grain is greater than 4 MPa. Water absorption and linear shrinkage are reduced by the increase with the addition of brewer's spent grain from all percentages in adobe. Due to the insulating properties of the cellulose in the waste, adding brewer's spent wastes grain reduces the thermal conductivity of adobes. Between 2 and 4 wt % of brewer's spent grain yields good mechanical and physical characteristics. These composites can be used to build habitats in the sub-Saharan region because of their low heat conductivity, resistance to water erosion, and good compressive strength of adobes using brewer's leftover grain.

Abbreviations

| | |
|-----|------------------------|
| PSG | Profil Salak Gakcle |
| PSE | Profil Salak Engrenage |
| PSL | Katoual |
| XRD | X-Ray Diffraction |
| IR | Infra-red |
| CE | Coefficient of Erosion |
| CA | Abrasion Coefficient |
| WL | Liquid Limit |
| WP | Plastic Limit |
| PI | Plasticity Index |
| MPa | Mega Pascal |

Author Contributions

Viviane Bakaïné Djaoyang: Conceptualization, Formal Analysis, Methodology, Writing, Resources

Maxime Dawoua Kaoutoing: Formal Analysis, Methodology

Bertin Pagna Kagonbé: Formal Analysis, Methodology

Colbert Babé: Formal Analysis, Methodology

Bernard kola: Formal Analysis, Methodology

Noël Djongyang: Review & editing

Conflicts of Interest

The authors declare no conflicts of interest.

References

- [1] P. Doat, A. Hays, H. Houben, S. Matuk, F. Vitoux, *Construire en Terre*, Editions Alternative et Parallèles, Paris, 1979.
- [2] M. Ouedraogo, K. Dao, Y. Millogo, J. E. Aubert, A. Messan, M. Seynou, L. Zerbo, M. Gomina, Physical, thermal and mechanical properties of adobes stabilized with fonio (*Digitaria exilis*) straw, *J. Build. Eng.* 23 (2019) 250–258, <http://dx.doi.org/10.1016/j.jobe.2019.02.005B>
- [3] Emad, Z. Gholamreza, S. Ezzatollah, B. Alireza, Global strategies and potentials.
- [4] H. Niroumand, M. F. M. Zain, M. Jamil, Various types of earth buildings, *Procedia – Soc. Behav. Sci.* 89 (2013) 226–230, <https://doi.org/10.1016/j.sbspro.2013.08.839>
- [5] S. V. Joshi, L. T. Drzal, A. K. Mohanty, S. Arora, *Compos. Part A Appl. Sci. Manufacturing* 35 (2004) 371–376.
- [6] D. Shah, *Compos. B Eng.* 52 (2013) 172–181H.
- [7] M. Cataldo-Born, G. Araya-Letelier, C. Pabón, Obstacles and motivations for earthbag social housing in Chile: energy, environment, economic and codes implications, *Rev. la Construcción. J. Constr.* 15(3) (2016) 17–26.
- [8] S. Deboucha, R. Hashim, A review on bricks and stabilized compressed earth blocks, *Sci. Res. Essays* 6(3) (2011) 499–506.
- [9] G. Calatan, A. Hegyi, C. Dico, C. Mircea, Experimental research on the recyclability of the clay material used in the fabrication of adobe bricks type masonry units, *Proc. Eng.* 181 (2017) 363–369.
- [10] M. Hall, Y. Djerbib, Rammed earth sample production: context, recommendations and consistency, *Constr. Build. Mater.* 18(4) (2004) 281–286.
- [11] S. Yetgin, Ö. Çavdar, A. Çavdar, The effects of the fiber contents on the mechanic properties of the adobes, *Constr. Build. Mater.* 22(3) (2008) 222–227.
- [12] M. Ali, A. Alabdulkarem, A. Nuhait, K. Al-Salem, Gino Iannace, R. Almuzaqer, A. Al-turki, F. Al-Ajlan, Y. Al-Mosabi, A. Al-Sulaimi, Thermal and acoustic characteristics of novel thermal insulating materials made of Eucalyptus Globulus leaves and wheat straw fibers, *J. Build. Eng.* 32 (November) (2020) 101452, <http://dx.doi.org/10.1016/j.jobe.2020.10145220-4-2020>
- [13] M. Ali, A. Alabdulkarem, On thermal characteristics and microstructure of a new insulation material extracted from date palm trees surface fibers, *Constr. Build. Mater.* 138(May) (2017) 276–284.
- [14] M. Ali, A. Alabdulkarem, A. Nuhait, K. Al-Salem, R. Almuzaqer, O. Bayaquob, H. Salah, A. Alsaggaf, Z. Algafri, Thermal analyses of loose agave, wheat straw fibers and agave/wheat straw as new hybrid thermal insulating materials for buildings, *J. Nat. Fibers* (2020), <http://dx.doi.org/10.1080/15440478.2020.1724232> Published online 7 Feb.
- [15] Mohamed Ali, Microstructure, thermal analysis and acoustic characteristics of calotropis procera (Apple of Sodom) fibers (DOI: 10.1080/ 15440478.2015.1029198), *J. Nat. Fibers* 13 (June (03)) (2016) 343–352, <http://dx.doi.org/10.1016/j.conbuildmat.2017.02.012>
- [16] Y. Elhamdouni, A. Khabbazi, C. Benayad, A. Dadi, O. I. Ahmad, Effect of fiber alfa on thermophysical characteristics of a material based on clay, *Energy Procedia* 74 (2015) 718–727.

- [17] M. Ouedraogo, K. Dao, Y. Millogo, M. Seynou, J. E. Aubert, M. Gomina, Influence des fibres de kenaf (*Hibiscus altissima*) sur les propriétés physiques et mécaniques des adobes, *J. Soc. Ouest.-Afr. Chim.* 043 (2017) 48–63.
- [18] Y. Millogo, J. E. Aubert, A. D. Séré, A. Fabbri, J. C. Morel, Earth blocks stabilised by cow-dung, *Mater. Struct.* 49 (2016) 4583–4594.
- [19] Y. Millogo, J. C. Morel, J. E. Aubert, K. Ghavami, Experimental analysis of Pressed Adobe Blocks reinforced with *Hibiscus cannabinus* fibers, *Constr. Build. Mater.* 52 (2014) 71–78.
- [20] Marwan, N. Uddin, Effect of banana fibers on the compressive and flexural strength of compressed earth blocks, *Buildings* 5 (2015) 282–296, <http://dx.doi.org/10.3390/buildings5010282>
- [21] B. Sorgho, P. Bressollier, B. Guel, L. Zerbo, R. Ouedraogo, M. Gomina, P. Blanchart, Etude des propriétés et mécaniques des géomatériaux argileux associant la décoction de *Parkia Biglobosa* (nééré), *C. R. Chim.* xxx (2016) 1–7.
- [22] H. Bal, Y. Jannot, S. Gaye, F. Demeurie, Measurement and modelisation of the thermal conductivity of a wet composite porous medium: laterite based bricks with millet waste additive, *Constr. Build. Mater.* 41 (2013) 586–593.
- [23] C. Babé, D. Kaoga Kidmo, A. Tom, R. R. Ngono Mvondo, R. Belinga Essama Boum, N. Djongyang, Thermomechanical characterization and durability of adobes reinforced with millet waste fibers (*sorghum bicolor*), <https://doi.org/10.1016/j.cscm.2020.e00422> Case Studies in Construction Materials 13 (2020) e00422.
- [24] S. I. Mussatto, M. Fernandes, G. J. M. Rocha, J. M. Órfão, J. A. Teixeira, I. C. Roberto Production, characterization and application of activated carbon from brewer's spent grain lignin, <https://doi.org/10.1016/j.biortech.2009.11.025> Bioresource Technology 101 (2010) 2450–2457.
- [25] S. I. Mussatto, Dragone, G., Roberto, I. C., 2006a. Brewer's spent grain: generation, characteristics and potential applications. *J. Cereal Sci.* 43, 1–14.
- [26] J. B. Suchel, 1972. La répartition des pluies et les régimes pluviométriques au Cameroun. *Doc. Géographie tropicale* 5 CEGET-CNRS. Talence, 287 p.
- [27] J. P. Temga, J. Maché, M. Balo, JP. Nguetnkam, D. L Bitom (2019) Ceramics applications of clay in Lake Chad Basin, Central Africa. *Appl Clay Sci* 171: 118–132H. M.
- [28] Y. Millogo, J. C. Morel, J. E. Aubert, K. Ghavami, Experimental analysis of pressed adobe blocks reinforced with *Hibiscus cannabinus* fibers, *Constr. Build. Mater.* 52 (2014) 71–78.
- [29] Y. Millogo, J. E. Aubert, D. A. Séré, A. Fabbri, J. C. Morel, Earth blocks stabilized by cow-dung, *Mater. Struct.* 49 (2016) 4583–4594.
- [30] K. Dao, M. Ouedraogo, Y. Millogo, J. E. Aubert, M. Gomina, Thermal, hydric and mechanical behaviors of adobes stabilized with cement, *Constr. Build Mater.* 158 (2018) 84–96.
- [31] J. Yvon, P. Garin, J. F. Delon, J. M. Cases, Valorisation des argiles kaolinitiques des Charentes dans le caoutchouc naturel, *Bull. Minéra* 105 (1982) 431–437.
- [32] B. P. Kagonbe, D. Tsozue, A. N. Nzeukou, S. Ngo Algin, P. Turgut Mineralogical, physico-chemical and ceramic properties of clay materials from Sekande and Gashiga (North, Cameroon) and their suitability in earthenware production <https://doi.org/10.1016/j.heliyon.2021.e07608>
- [33] X. P. AFNOR, P13-901 “Blocs de terre comprimée pour murs et cloisons: définitions-Spécifications-Méthodes d'essais-Conditions de réception,” (2001).
- [34] , D. S. Basga, D. Tsozué, J. P. Temga, J. Balna and J. P. Nguetnkam, "Land use impact on clay dispersion/flocculation in irrigated and flooded Vertisols from Northern Cameroon"! International Soil and Water Conservation Research, (2018) 237-244.
- [35] S. D. Basga, J. P. Temga, D. Tsozué and A. Gové, Erodibility of Vertisols in relation to agricultural practices along a toposequence in the Logone floodplain Soil and Environment, 39 (2020) 1-12 <https://doi.org/10.25252/SE/2020/101855>
- [36] Richer de Forges, A., Feller, C., Jamagne, M., & Arrouays D. (2008). Perdu dans le triangle de textures. *Etudes et gestion des Sols*, 15, 97-111.
- [37] H. Bamogo, M. Ouedraogo, I. Sanou, K. A. Jérémy, Ouedraogo, K. Dao, J. Aubert, Y. Millogo, Improvement of water resistance and thermal comfort of earth renders by cow dung: an ancestral practice of Burkina Faso, *Journal of Cultural Heritage* (2020) <https://doi.org/10.1016/j.culher.2020.04.009P>
- [38] D. Tsozué, N. A. Nzeukou, J. R. Maché, S. Loweh, N. Fagel, 2017, Mineralogical, physico-chemical and technological characterization of clays from Maroua (Far-North, Cameroon) for use in ceramic bricks production. *J Build Eng* 11: 17–24.
- [39] Chahi, A. and Petit D. (2002) Infrared Evidence of a Dioctahedral-Trioctahedral Sites Occupancy in Palygorskite. *Clay-sandClayMinerals*, 50, 306-313. <https://doi.org/10.1346/00098600260358067>
- [40] Nguetnkam, J. P., Kamga, R., Villiéras, F., Ekodeck, G. E., Yvon, J., 2008. Assessing the bleaching capacity of some Cameroonian clays on vegetable oils. *Appl. Clay Sci.* 39, 113–121.
- [41] Kagonbé, B. P., Tsozué, D., Nzeukou, A. N., Basga, S. D., Belinga, R. E., Likiby, B. and Ngos III, S. (2020a). Suitability of Lateritic Soils from Garoua (North Cameroon) in Compressed Stabilized Earth Blocks Production for Low-Cost Housing Construction. *Journal of Materials and Environmental Science*, 11, 658-669.
- [42] Kagonbé, P. B., Tsozué, D., Djépaze, II, Y., Nzeugang, N. A., Balo, M. B., Basga, D. S., & Ngos, III S. (2020b). Physical Characterization and Optimization of Fineness Moduli of Natural Sand from the North Region of Cameroon Used in Construction. *Journal of Sustainable Construction Materials and Technologies*, 5, 407-419. <https://doi.org/10.29187/jscmt.2020.45>

- [43] Tsozué, N. A. Nzeukou, B. Pagna Kagonbé, A. Balo, J. R. Maché, D. L. Bitom, N. Fagel Genesis and assessment of clay materials suitability for earthenware production in northern Cameroon *Arabian Journal of Geosciences* (2022) 15: 1376 <https://doi.org/10.1007/s12517-022-10603-7> 2022.
- [44] Iyammi, B. M., Tchede, L. Y., Alarba, S. T. A., Mache, J. R. and Mominou, N. (2023) Physico-Chemical, Mineralogical Characterization, and Ceramic Properties of Clay Materials from South Mindif (Far North, Cameroon). *JMSTAdvancesJournal*, 5, 13-26. <https://doi.org/10.1007/s42791-023-00047-9>
- [45] E. Yanné, A. A Oumarou, B. D. Nde, R. Danwe; 2018; Physico-chemical and mineralogical characterization of two clay materials of the far north region of Cameroon (Makabaye, Maroua). *Adv Mater Phys Chem* 8: 378–386.
- [46] . S. Talibi, J. Page, C. Djelal, L. Saadi; Impact of treated red-algae fibers in physic-mechanical behavior of compressed earth brick for construction; *European journal of environmental and civil engineering*, <https://doi.org/10.1080/19648189> (2024).
- [47] Laborel-Préneron, J. E. Aubert, C. Magniont, C. Tribout, A. Bertron, Plant aggregates and fibers in earth construction materials: a review, *Constr. Build. Mater.* 11 (2016) 719–734.
- [48] H. Omrani, L. Hassini, A. Benazzouk, H. Beji, A. ELcfsi Elaboration and characterization of clay-sand composite based on *Juncus acutus* fibers, *Construction and Building Materials* 238 (2020) 117712 <https://doi.org/10.1016/j.conbuildmat.2019.117712> 2020.
- [49] P. Zak, T. Ashour, A. Korjenic, S. Korjenic, W. Wu, The influence of natural reinforcement fibers, gypsum and cement on compressive strength of earth bricks materials, *Constr. Build. Mater.* 106 (2016) 179–188.
- [50] H. Danso, D. B. Martinson, M. Ali, John B. Williams, Physical, mechanical and durability properties of soil building blocks reinforced with natural fibers, *Constr. Build. Mater.* 101 (2015) 797–809.
- [51] A. Laborel-Preneron, C. Magniont, J.-E. Aubert, Hygrothermal properties of unfired earth bricks: effect of barley straw, hemp shiv and corn cob addition, *Energy Build.* (2018), <http://dx.doi.org/10.1016/j.enbuild.2018.08.021>
- [52] T. Ashour, A. Korjenic, S. Korjenic, W. Wu, Thermal conductivity of unfired earth bricks reinforced by agricultural waste with cement and gypsum, *Energy Build.* 135 (2017) 109–118. C. N.
- [53] H. Bal, Y. Jannot, N. Quenette, A. Chenu, S. Gaye, Water content dependence of the porosity, density and thermal capacity of laterite based bricks with millet waste additive, *Constr. Build. Mater.* 31 (2012) 144–150.
- [54] H. Bal, Modélisation et mesure de propriétés thermiques d'un milieu poreux humide: brique de latérite avec gousse de mil, thèse de doctorat de Chekh Anta Diop de Dakar, 2020.
- [55] Yves Jannot, Métrologie thermique, Laboratoire d'Energétique et de Mécanique Théorique et Appliquée (LEMTA), Centre National de la Recherche Scientifique, Nancy-Université, 2011.
- [56] G. Minke, Building with Earth. Design and Technology of a Sustainable Architecture (Text Book) Birkhaeser, Publishers for Architecture, Basel, Berlin, Boston, '2006).
- [57] P. M. Touré, Vincent Sambou, Mactar Faye, Ababacar Thiam, Mamadou Adj, Dorothé Azilnon, Mechanical and hygro-thermal properties of compressedstabilized earth bricks (CSEB), *J. Build. Eng.* 13 (2017) 266–271.
- [58] Organisation Régionale Africaine de Normalisation, Ed. Blocs de terre comprimée: norme. Technologie no 11, CDI et CRA-Terre-EAG, Belgique, mars, (1998).
- [59] Villamizar, V. S. Araque, C. A. R. Reyes, R. S. Silva, Effect of the addition of coal-ash and cassava peels on the engineering properties of compressed earth blocks, *Constr. Build. Mater.* 36 (2012) 276–286, <http://dx.doi.org/10.1016/j.conbuildmat.2012.04.056>
- [60] H. Bamogo, M. Ouedraogo, I. Sanou, K. Amed J. Ouedraogo, K. Dao, J. Aubert, Y. Millogo, Improvement of water resistance and thermal comfort of earth renders by cow dung: an ancestral practice of Burkina Faso, (2020) Elsevier Masson <https://doi.org/10.1016/j.culher.2020.04.009> 1296-2074/© SAS.